

REPORT

Yorkie and JNK revert syncytial muscles into myoblasts during Org-1-dependent lineage reprogramming

Christoph Schaub, Marcel Rose, and Manfred Frasch

Lineage reprogramming has received increased research attention since it was demonstrated that lineage-restricted transcription factors can be used in vitro for direct reprogramming. Recently, we reported that the ventral longitudinal musculature of the adult *Drosophila* heart arises in vivo by direct lineage reprogramming from larval alary muscles, a process that starts with the dedifferentiation and fragmentation of syncytial muscle cells into mononucleate myoblasts and depends on Org-1 (*Drosophila* Tbx1). Here, we shed light on the events occurring downstream of Org-1 in this first step of transdifferentiation and show that alary muscle lineage-specific activation of Yorkie plays a key role in initiating the dedifferentiation and fragmentation of these muscles. An additional necessary input comes from active dJNK signaling, which contributes to the activation of Yorkie and furthermore activates dJun. The synergistic activities of the Yorkie/Scalloped and dJun/dFos transcriptional activators subsequently initiate alary muscle fragmentation as well as up-regulation of *Myc* and *piwi*, both crucial for lineage reprogramming.

Introduction

The somatic musculature of the fruit fly Drosophila melanogaster as well as that of vertebrates is composed of terminally differentiated striated muscle fibers that are built by long syncytial cells. They arise during embryonic development by fusion of mononucleate muscle progenitor cells and acquire individual muscle identities that define their particular features, e.g., their shape, innervation, and attachment sites (Dobi et al., 2015). During metamorphosis, the building of the adult musculature involves a radical reconstruction of the multinucleated, striated body wall musculature. The vast majority of larval body wall muscles become histolysed and disappear, and almost all adult muscles are then newly built from stem cell-like adult muscle precursor cells (Gunage et al., 2017). However, some specific larval muscles escape histolysis and are remodeled into adult muscles, as is the case for the formation of the indirect flight muscles (Dutta and VijayRaghavan, 2006).

Recently, we discovered a new mode of larval-to-adult muscle remodeling, which applies for the development of syncytial muscles associated with the adult heart, the so-called ventral heart-associated longitudinal muscles (ventral longitudinal musculature; VLM), from a different type of larval syncytial muscles, called alary muscles (AMs; Schaub et al., 2015).

The formation of the VLMs resembles a process of direct lineage reprogramming, which includes dedifferentiation and fragmentation of syncytial AMs (Fig. 1, A and B) into mononucleate myoblasts, called AM-derived cells (AMDCs; Fig. 1, A and C). The AMDCs are reprogrammed into muscle progenitors that subsequently undergo fusion with myoblasts from other sources again and redifferentiate into the VLMs (Fig. 1, A and D; and Video 1). Important components of the genetic program that regulate the development of VLMs from AMs are the T-box factor Org-1 (Drosophila Tbx1) and its direct target, the LIM homeodomain factor Tup (Drosophila Islet1), which are instrumental in initiating the dedifferentiation process. The spatial restriction of the dedifferentiation process is mediated by the action of Hox genes, in particular Ubx, which is restricted to the anterior three pairs of AMs (LaBeau et al., 2009). Likewise, the temporal regulation is mediated by stage-specific hormonal inputs by the ligand-bound nuclear receptor of the steroid molting hormone ecdysone (Schaub et al., 2015). However, the events that exert dedifferentiation and fragmentation of AMs as well as redifferentiation of the AMDCs downstream of Org-1 and Tup are as yet unknown.

Here we report that the AM lineage-specific activity of Yorkie (Yki), the transcriptional effector of the Hippo pathway

Friedrich-Alexander-Universität Erlangen-Nürnberg, Department of Biology, Division of Developmental Biology, Erlangen, Germany.

Correspondence to Manfred Frasch: manfred.frasch@fau.de; Christoph Schaub: christoph.schaub@fau.de.

© 2019 Schaub et al. This article is distributed under the terms of an Attribution–Noncommercial–Share Alike–No Mirror Sites license for the first six months after the publication date (see http://www.rupress.org/terms/). After six months it is available under a Creative Commons License (Attribution–Noncommercial–Share Alike 4.0 International license, as described at https://creativecommons.org/licenses/by-nc-sa/4.0/).





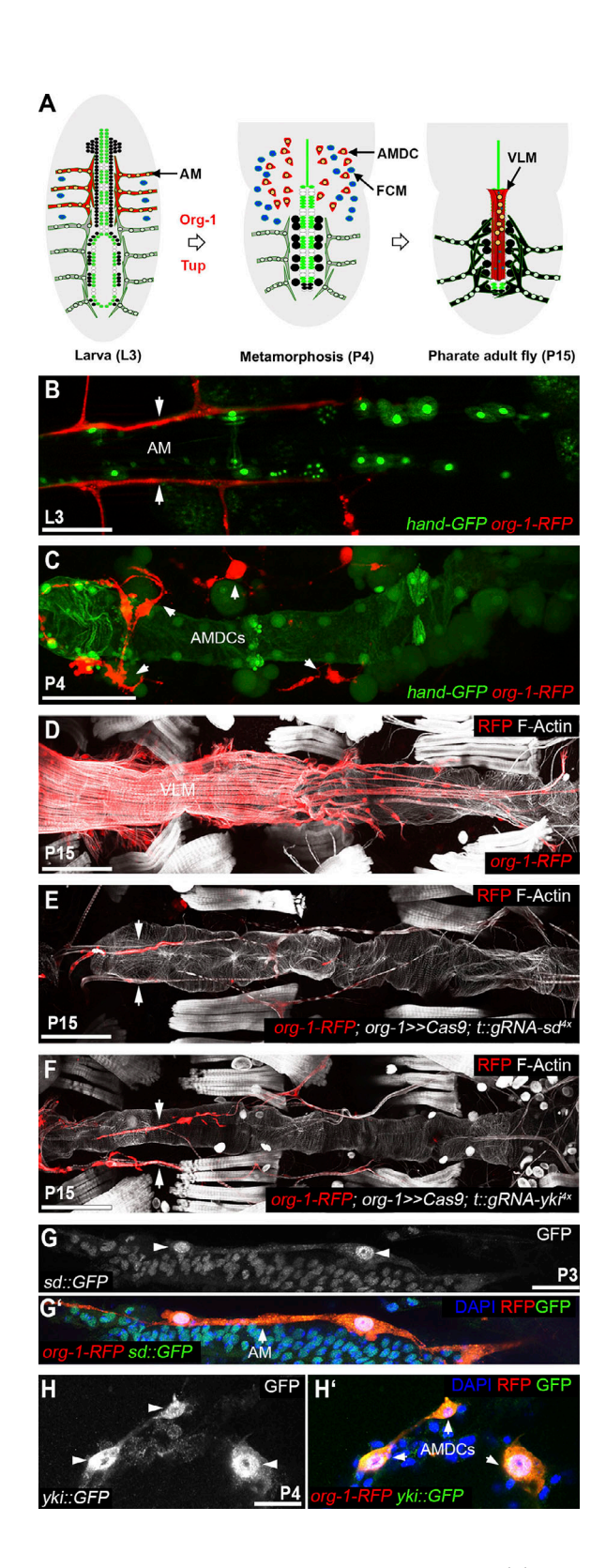


Figure 1. Sd and Yki are required for AM dedifferentiation. (A) Schematic depiction of AM lineage reprogramming during metamorphosis. After onset of metamorphosis, Org-1 and Tup expression is initiated specifically in the three anterior pairs of AMs, thus triggering dedifferentiation of the syncytial AMs into mononucleate AMDCs. Each of the mononucleate AMDCs serves as a muscle founder cell, fuses with fusion-competent myoblasts (FCMs), and forms a syncytial muscle cell. The newly formed syncytia migrate to the ventral anterior part of the heart tube and differentiate into the VLM. (B and C) Ex vivo live imaging of dissected pupae carrying the org-1-HN18-RFP

and coactivator of the transcription factor Scalloped (Sd), plays a key role in initiating AM dedifferentiation and fragmentation downstream of Org-1/Tup. We demonstrate that active Drosophila JNK (dJNK) signaling is indispensable for AM fragmentation by contributing to both the activation of Yki and the activation of Drosophila Jun (dJun), thus leading to the formation of the Yki/Sd and dJun/dFos (AP-1) effector complexes. The molecular programs that are initiated by the synergistic activities of these transcriptional activators induce AM dedifferentiation and lead to the activation of Myc and piwi, which are crucial for different aspects of AM lineage reprogramming. Together, our results show that derepression of Yki downstream of lineage-specific transcription factors, in concert with active dJNK signaling, mediates lineage plasticity and initiates a cell fate switch during a naturally occurring process of muscle lineage reprogramming.

Results and discussion

Yki and Sd promote AM dedifferentiation

In a recently performed AM-specific in vivo RNAi screening, we identified scalloped (sd) and yorkie (yki) as crucial genes for VLM formation. org-1-GAL4-mediated knockdown of sd or yki within the AMs by either cell type specifically induced RNAi (Fig. S1, B and C) or CRISPR (Fig. 1, E and F; and Table S1) abolishes VLM formation, and leads to the presence of org-1-RFP-positive muscles that may represent remnants of the larval AMs. Yesassociated protein (YAP), the mammalian homologue of Yki, can function as coactivator for several transcription factors including members of the TEA domain family (TEAD)/transcriptional enhancer family (TEF). In Drosophila, Yki forms a complex with the single TEAD/TEF family member Sd that can activate transcriptional targets after nuclear translocation (Goulev et al., 2008; Wu et al., 2008; Zhao et al., 2008). Visualization of a GFP-tagged version of the endogenous protein clearly demonstrates that Sd is located in the nuclei of the syncytial orq-1-RFP-positive AM cells (Fig. 1, G and G'). Although we were not able to detect nuclear GFP-tagged Yki protein expressed under endogenous control (Yki::GFP) in intact AMs, distinct nuclear accumulation was apparent during fragmentation of the AMs into org-1-RFP-positive AMDCs (Fig. 1, H and H'). Live imaging confirmed that the phenotypes in yki knockdown backgrounds

(org-1-RFP) and hand-GFP reporter constructs. In larval stage L3, org-1-RFP expression is seen in the first three pairs of AMs (B; arrows) that initiate dedifferentiation in pupal stage P4 (C) and fragment into mononucleated progenitor-like cells, AMDCs (arrows). (D) org-1-RFP drives reporter expression in the VLM attached to the heart of a pharate adult stage P15. (E and F) Induction of CRISPR in the AMs with HN39-org-1-GAL4 (org-1-GAL4) against sd $(org-1>>Cas9; t::qRNA-sd^{4x}; E)$ or yki $(org-1>>Cas9; t::qRNA-yki^{4x}; F)$ blocks VLM formation and prevents AM fragmentation during metamorphosis into pharate adult stage P15 (arrows). (G and H) Visualization of the org-1-RFP lineage marker and GFP-tagged versions of Sd (Sd::GFP) and Yki (Yki::GFP). Sd::GFP can be detected at pupal stage P3 in the nuclei (arrowheads) of the syncytial AM (G and G'; arrow) whereas Yki::GFP can be detected during induction of AM fragmentation in the nuclei (H and H'; arrowheads) of the forming AMDCs (arrows) during pupal stage P4. Scale bars in A-E: 100 µm; F and G: 10 µm. Actin is visualized with phalloidin; DNA is visualized with DAPI.



result from the inability of the AMs to dedifferentiate into AMDCs (Video 2). Thus, we propose that Yki and Sd are crucial for the initiation of AM transdifferentiation.

Derepression of Yki mediates AM lineage reprogramming

The evolutionarily conserved Hippo pathway has been identified as one of the key inputs regulating Yki/YAP activity, particularly in the control of organ size via calibrating cell proliferation and apoptosis. Its core is represented by a kinase cascade consisting of Hippo (Hpo; Harvey et al., 2003; Jia et al., 2003; Pantalacci et al., 2003; Udan et al., 2003) and Warts (Wts) that phosphorylates Yki, thereby inhibiting its nuclear translocation and its function as a transcriptional coactivator of Sd (Huang et al., 2005; Goulev et al., 2008; Wu et al., 2008; Zhao et al., 2008). To dissect a potential role of Hpo signaling during AM lineage reprogramming, we overexpressed various Yki and Hpo constructs (Fig. 2 A) with org-1-GAL4. Nonphosphorylatable Yki (YkiS^{168A}) did not cause any effect in this assay (Fig. 2, A and C). Strikingly, however, forced expression of constitutively active Hpo (UAS- $Hpo^{\Delta C}$, an N-terminal fragment possessing the Ste20 kinase domain but not the regulatory domains) completely abrogates AM transdifferentiation (Fig. 2, B and D). Since this effect is not observed upon expression of the same deletion construct carrying an inactive Ste20 kinase domain (UAS- $Hpo^{\Delta C.K7IR}$; Fig. 2 E), of full-length Hpo (UAS-Hpo; Fig. 2 F), or of its regulatory C-terminal part (UAS-Hpo $^{\Delta N}$; Fig. 2 G) in the AMs, this strongly suggests that activated Hpo signaling blocks the induction of lineage reprogramming in the AMs. To prove that Hpo pathway-mediated suppression of Yki function provokes the observed phenotypes in $Hpo^{\Delta C}$ overexpression backgrounds, we coexpressed it together with phosphorylationresistant, constitutively active Yki (UAS-ykiS168A). This caused a significant rescue of VLM formation (P ≤ 0.0001; Fig. 2, B and H), thus strengthening our hypothesis that inactivation of the Hpo kinase cascade may lead to the activation of the Yki/Sd transcriptional activator complex that is critical for inducing AM reprogramming. Strikingly, by overexpressing Hpo-insensitive Yki^{S168A} in a genetic background in which we induced RNAi against org-1 or its direct target tup (Schaub et al., 2015), we observed that constitutively active Yki achieves a significant rescue of VLM formation (org-1 P \leq 0.01, tup P \leq 0.0001; Fig. 2, B and I-L). Taken together, these results are fully consistent with a mechanism in which Org-1-dependent inactivation of the Hippo pathway and concomitant activation of Yki/Sd target gene programs are needed to trigger AM dedifferentiation into AMDCs.

In a first effort to explore possible links between Org-1 and Hippo signaling during lineage reprogramming, we tested additional known inputs into this pathway. In recent work, it was proposed that atypical PKC (aPKC) signaling can regulate the nuclear outputs of the Hippo cascade either positively, namely by dislocating and down-regulating Hippo kinase activity (Grzeschik et al., 2010), or in the case of mouse intestinal cells, negatively, namely by directly phosphorylating YAP via the aPKC member PKCζ (Llado et al., 2015). To test if aPKC activity plays a role in Hpo regulation during AM transdifferentiation, we expressed a membrane-tethered, dominant-negative form of aPKC (UAS-aPKCCAAX-DN) and a constitutively active aPKC

deletion construct ($UAS-aPKC^{\Delta N}$) via org-1-GAL4. Down-regulation of aPKC activity does not have any impact on VLM formation and thus does not appear to cause increased Hpo activity in this context (Fig. 3 B). By contrast, the presence of the constitutively active form of aPKC abrogates VLM formation and AM lineage reprogramming, which could be due to increased Hpo and/or decreased Yki activity (Fig. 3 C). In line with this possibility, the loss of VLM formation in the aPKC gain-of-function genetic background can be rescued significantly by the coexpression of phosphorylation-resistant Yki ($P \le 0.0001$; Fig. 3, D and G). These results support a model in which aPKC signaling is involved in the upstream regulation of Yki activity and needs to be inactive during AM transdifferentiation.

JNK signaling is required for AM lineage reprogramming

Since it has been shown that there is a functional link between the activation of JNK signaling and down-regulation of Hpo pathway signaling (Sun and Irvine, 2013), we next asked if Basket (Bsk, dINK) activity is required for AM lineage reprogramming. To address this question, we overexpressed a dominant-negative form of dJNK (UAS-bskDN) in the AMs with org-1-GAL4, which resulted in the abolishment of VLM formation (Fig. 3 E). Interestingly, coexpression of BskDN and phosphorylation-resistant Yki^{S168A} leads to a significant rescue of VLM differentiation (P ≤ 0.0001; Fig. 3, F and G), which indicates that active dJNK normally acts in promoting nuclear Yki, which possibly also in this context involves down-regulating the Hippo pathway kinases. However, the VLM morphology in the rescued phenotypes is severely disturbed, pointing toward additional inputs from dINK signaling into AM lineage reprogramming. As a key component of the JNK pathway, dJNK phosphorylates the transcription factor Jun-related antigen (Jra, dJun) that, together with Kayak (Kay, dFos), subsequently forms a heterodimeric protein complex, AP-1, which represents the transcriptional effector of JNK signaling (Kockel et al., 2001). By characterizing the expression pattern of an in vivo AP-1 sensor construct (TRE-GFP) during metamorphosis, we demonstrate TRE-GFP expression in orq-1-RFP-positive AMDCs (Fig. 3, H and H'), thus implying that AP-1 targets are bound and activated during AM dedifferentiation. Importantly, down-regulation of either dJun or dFos in the AMs by RNAi (Fig. S1, D and E) or by inducible CRISPR (Fig. 3, I and J; and Table S1) abolishes VLM formation and interferes with AM fragmentation, thus pointing to a crucial function of AP-1 during AM transdifferentiation.

AM lineage reprogramming requires Myc and piwi

Target genes of Yki have been mainly identified upon Yki hyperactivation or ectopic expression in imaginal discs. These experiments identified *Myc* as a transcriptional target of Yki, and it was shown that both work together in regulating proliferation and growth in epithelial imaginal cells (Neto-Silva et al., 2010; Ziosi et al., 2010). Down-regulation of *Myc* via inducible RNAi or CRISPR during AM transdifferentiation strongly interferes with VLM formation and AM reprogramming (Fig. S1 F, Fig. 4 B, and Table S1). Accordingly, live imaging demonstrated that upon RNAi-mediated Myc knockdown, AM dedifferentiation and fragmentation is severely impaired (Video 3), pointing



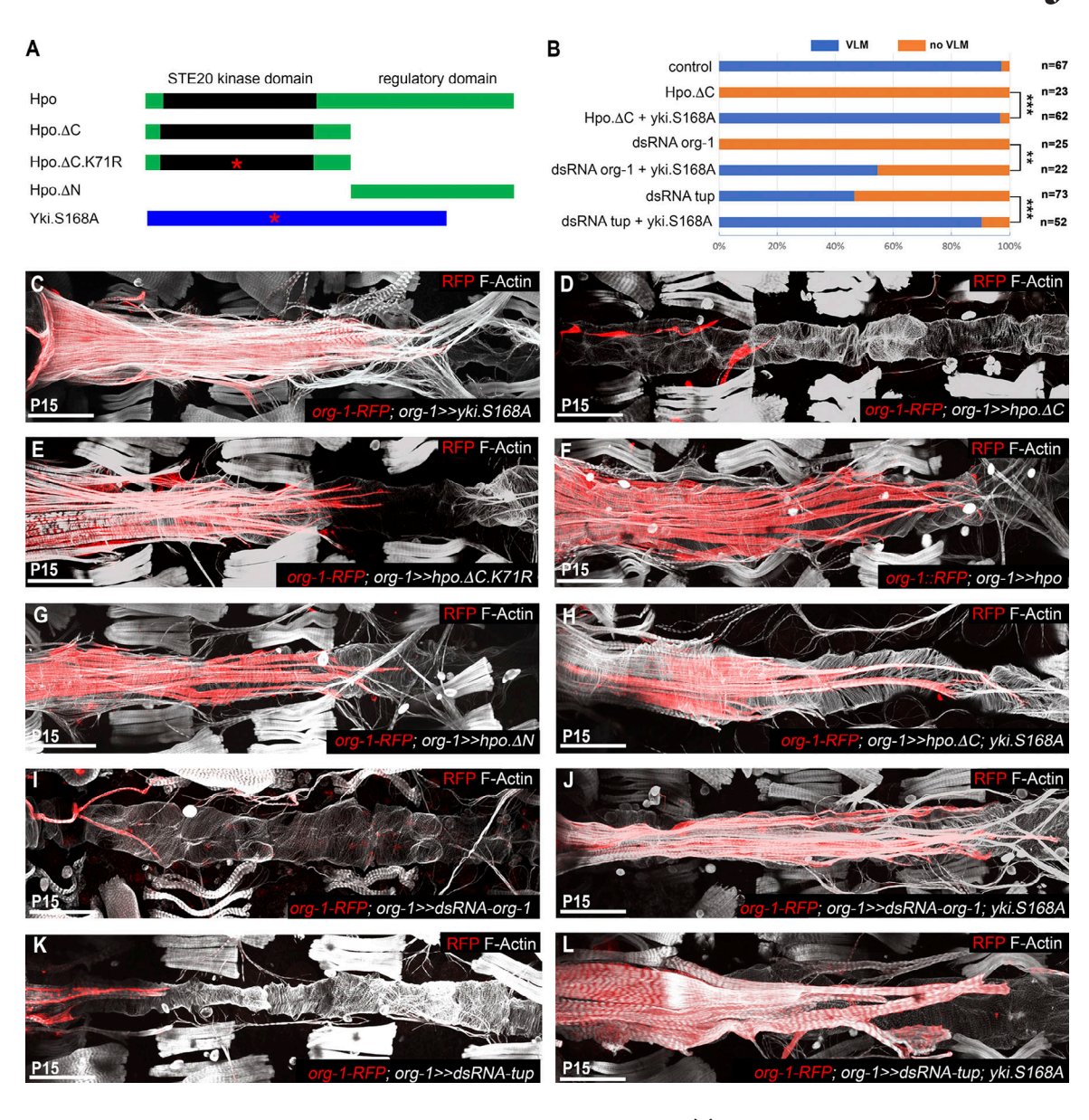


Figure 2. **Org-1-dependent derepression of Yki is needed for AM lineage reprogramming.** (**A**) Schematic drawings of Hpo and Yki constructs used for forced expression. Asterisks indicate positions of amino acid exchanges. (**B**) Frequencies of observed VLM differentiation in pharate adult stages P15 in the respective genetic backgrounds. n, number of animals phenotypically classified. Coexpression of Yki^{S168A} can significantly rescue the phenotypes provoked by forced expression of Hpo^{ΔC} (n = 62, ***, $P \le 0.001$) as well as the phenotypes induced by RNAi against Org-1 (n = 22, **, $P \le 0.001$) and Tup (n = 52, ***, $P \le 0.001$) and Tup (n = 52, ***, $P \le 0.001$). (**C**) Forced expression of phosphorylation-resistant Yki^{S168A} (org-1>>yki.S168A) with org-1-GAL4 does not provoke a VLM phenotype. (**D**) Forced expression of the N-terminal part of Hpo containing a functional STE20 kinase domain ($org-1>>hpo.\Delta C$) disrupts VLM formation and AM fragmentation. (**E–G**) Forced expression with org-1-GAL4 of the N-terminal part of Hpo containing a dead STE20 kinase domain ($org-1>>hpo.\Delta C.K71R$; E), full-length Hpo (org-1>>hpo. F), or an N-terminally truncated version of Hpo ($org-1>>hpo.\Delta N$; G) does not provoke a significant VLM phenotype. (**H**) VLM formation and AM lineage reprogramming can be partially rescued by coexpression of Yki^{S168A} in a Hpo^{ΔC} background ($org-1>>hpo.\Delta C$; yki.S168A). (**I and K**) Induction of RNAi with org-1-GAL4 against org-1 (org-1>>dsRNA-org-1; I) or tailup (org-1>>dsRNA-tup; K) disrupts VLM formation and AM lineage reprogramming. (**J and L**) Coexpression of Yki^{S168A} leads to the partial rescue of the phenotypes induced by the RNAi against either org-1 (org-1>>dsRNA-org-1; yki.S168A; I) or org-1>>dsRNA-tup; yki.S168A; L). Actin is visualized with phalloidin. Scale bars: 100 μm.

toward a crucial role for Myc in the initiation of AM reprogramming. The analysis of the expression pattern of a GFP-tagged version of Myc under endogenous control (Myc::GFP) during AM lineage reprogramming revealed that it can be detected, like Yki::GFP, in the nuclei of the AMDCs shortly after the initiation of syncytial AM fragmentation (Fig. 4, C and C'). Notably, the induction of Myc::GFP expression can be suppressed by forced expression of constitutively active Hpo ($UAS-Hpo^{\Delta C}$) with

org-1-GAL4 in the AMs (Fig. 4, D and D'; and Table S1), implicating Myc as a Yki target during AM lineage reprogramming.

Another target gene that has been identified upon Yki overexpression in *Drosophila* imaginal discs is *piwi* (Zhang et al., 2015). Down-regulation of *piwi* during AM transdifferentiation via inducible RNAi provokes loss of VLM formation (Fig. 4 E and Table S1). Live imaging revealed that upon *piwi* knockdown, the anterior, *org-1-RFP*-positive AMs do dedifferentiate and



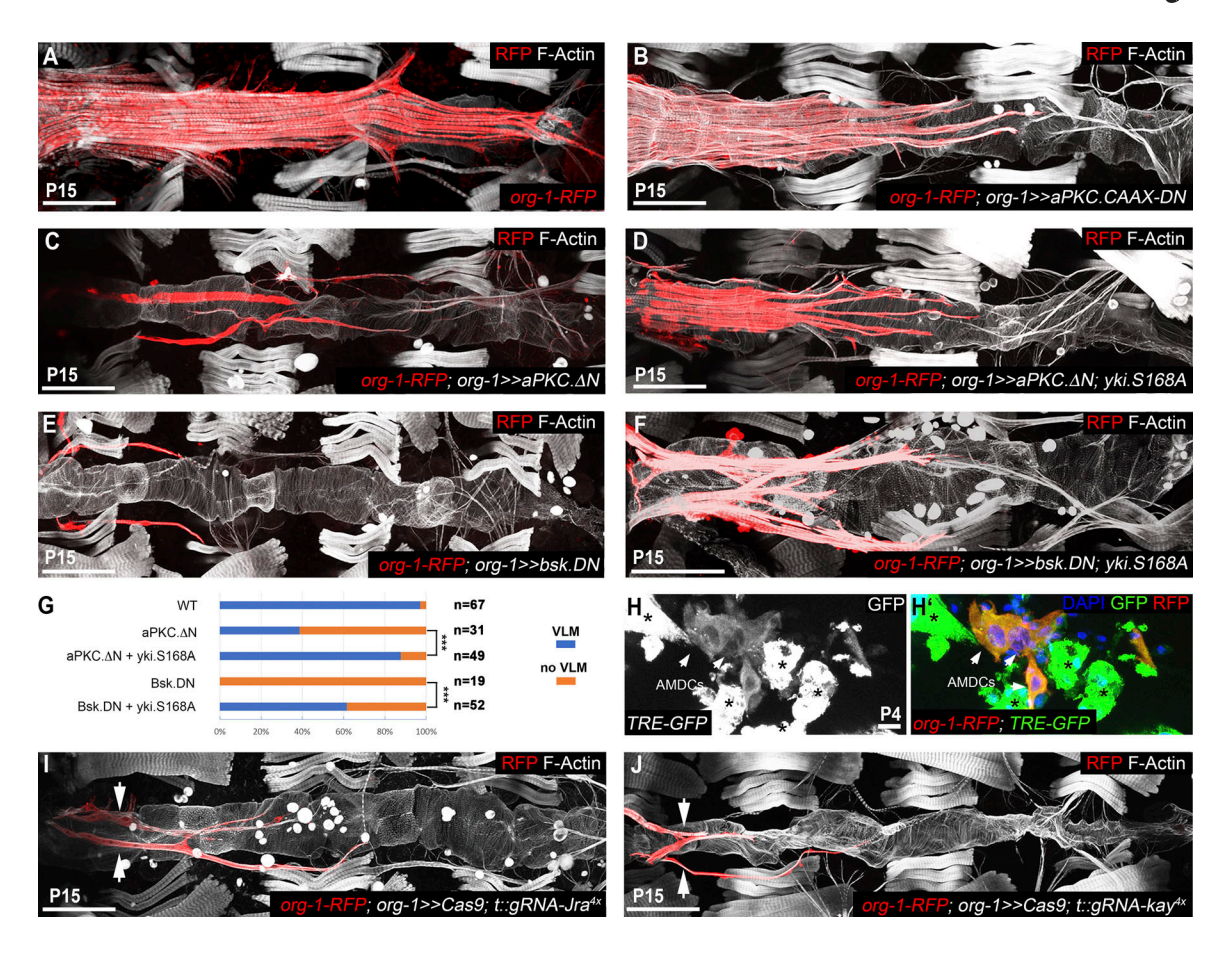


Figure 3. The transcriptional effectors of the Hippo and dJNK pathways act synergistically to induce AM fragmentation. (A) org-1-RFP and phalloidin mark the VLM in pharate adult stage P15. (B) Forced expression of a membrane-tethered version of dominant-negative aPKC (org-1>>aPKC.CAAX.DN) with org-1-GAL4 has no effect on AM reprogramming. (C) Induction of a constitutive active form of aPKC (org-1>> $aPKC.\Delta N$) with org-1-GAL4 disrupts VLM differentiation and AM transdifferentiation. (D) The lost VLM phenotype in an aPKC gain-of-function background can be partially rescued by coexpression of phosphorylation-resistant Yki^{S168A} (org-1>> $aPKC.\Delta N$; yki.S168A). (E) org-1-GAL4-mediated induction of a dominant-negative version of dJNK (org-1>>bsk.DN) leads to abolishment of VLM differentiation and AM transdifferentiation. (F) Coexpression of Yki^{S168A} in dJNK^{DN} background (org-1>>bsk.DN; yki.S168A) can rescue formation of VLM fibers, but there are fewer than in wildtype, and the morphology of the VLM is severely disrupted. (G) Frequencies of observed VLM differentiation in the different genetic backgrounds. n, number of animals phenotypically classified. Coexpression of Yki^{S168A} can significantly rescue the phenotypes provoked by forced expression of aPKC^{ΔN} (n = 49, ***, $P \le 0.001$) and dJNK^{DN} (n = 52, ***, $P \le 0.001$). (H and H') The in vivo AP-1 sensor TRE-GFP is activated in org-1-RFP-positive AMDCs (arrows) and (even more strongly) in org-1-RFP-negative apoptotic muscle cells (asterisks) at pupal stage P4. (I and J) Induction of CRISPR in the AMs with org-1-GAL4 against dJun [Jra]; org-1>>Cas9; $t::gRNA-Jra^{4x}$; I) or dFos [$t::gRNA-Jra^{4x}$; J) blocks VLM differentiation and AM fragmentation (arrows). Scale bars in A-F, I, and J: 100 μm; H: 10 μm. Actin is visualized with phalloidin; DNA is visualized with DAPI.

fragment into AMDCs, but AM transdifferentiation is arrested at this stage (Video 4). An endogenously controlled, GFP-tagged version of Piwi (Piwi::GFP) is not yet detectable in syncytial AMs and AMDCs during AM fragmentation but is expressed at high cytoplasmic levels during reprogramming of the AMDCs into the VLM progenitor cells (Fig. 4, F-G'). Like Myc::GFP, piwi::GFP activation is suppressed by forced expression of constitutively active Hpo ($UAS-Hpo^{\Delta C}$) with org-1-GAL4 in the AMs (Fig. 4, H and H'; and Table S1). These data suggest an important role of Piwi during the reprogramming of the AMDCs into the progenitor cells of the VLMs and identifies piwi as another Yki target during AM lineage reprogramming.

Taken together, these observations implicate *Myc* and *piwi* as important examples of targets that may be activated by the synergistic activities of Yki/Sd and AP-1, which in turn are required for mediating downstream effects of the Hippo and JNK cascades during this naturally occurring reprogramming process (Fig. 5).

Reversion of terminally differentiated states involves active JNK and inactive Hippo kinases

Although syncytial muscles are often considered a paragon of terminally differentiated cells, there are rare examples where skeletal muscle cells are induced to dedifferentiate and fragment into muscle progenitor cells, either by forced treatment or during a natural process as for the anterior *Drosophila* AMs (Odelberg et al., 2000; McGann et al., 2001; Jung and Williams, 2011; Sandoval-Guzmán et al., 2014; Schaub et al., 2015; Frasch, 2016). Our results herein reveal that effectors of the JNK and Hpo signaling pathways drive the lineage-specific dedifferentiation and fragmentation of syncytial AM cells into mononucleate myoblasts. With regard to muscles, JNK function in *Drosophila* has been associated with myonuclear positioning and visceral muscle-intrinsic left-right asymmetry (Taniguchi et al., 2007; Schulman et al., 2014), whereas Yki activity was described to be required for muscle growth during late pupal stages (Kuleesha



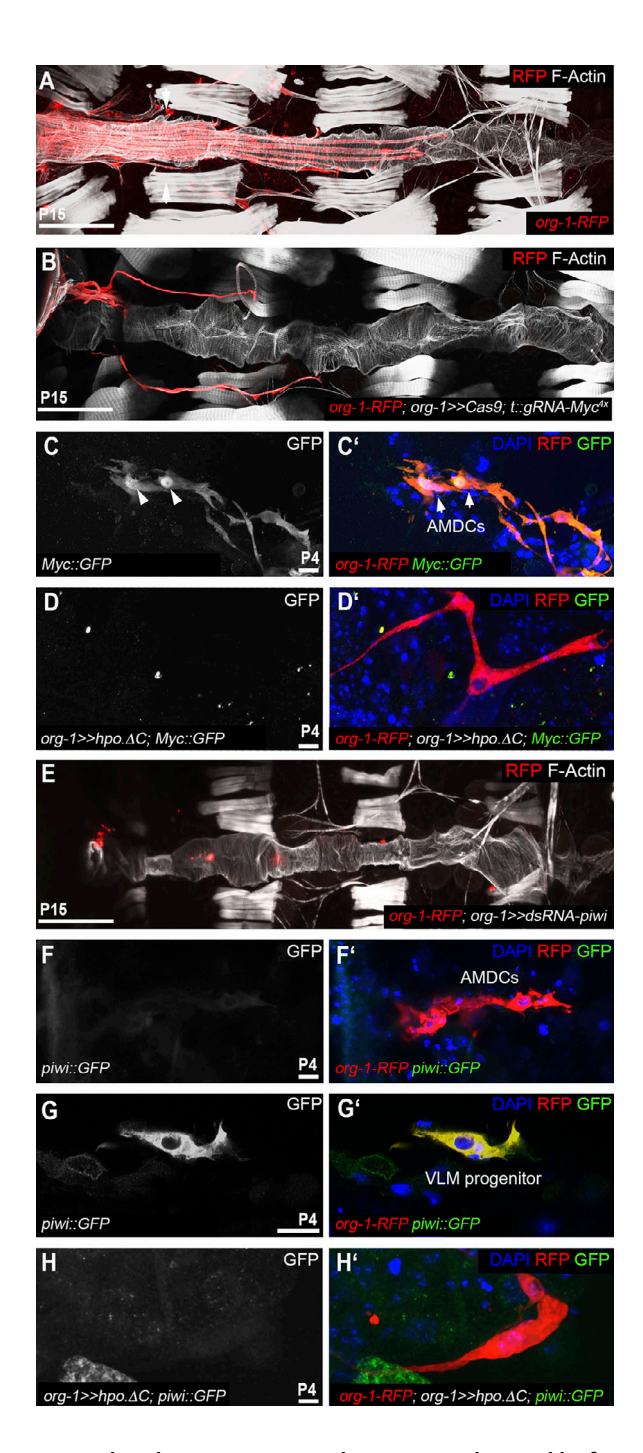


Figure 4. The Yki targets Myc and Piwi are indispensable for reprogramming of the AM lineage. (A) org-1-RFP and phalloidin mark the VLM. (B) Induction of CRISPR in the AMs with org-1-GAL4 against Myc (org-1>>Cas9; t::qRNA-Myc4x) abolishes VLM differentiation and blocks AM dedifferentiation. (C and D) Expression of a GFP-tagged Myc (Myc::GFP) can be detected in the nuclei (arrowheads) of the AMDCs (arrows) shortly after AM fragmentation (C and C'), but is suppressed by forced expression of constitutive active Hpo with org-1-GAL4 (org-1>>hpo.ΔC) in pupae at stage P4 (D and D'). (E) Induction of RNAi in the AMs with org-1-GAL4 against piwi (org-1>>dsRNA-piwi) abolishes VLM differentiation. (F and G) Visualization of org-1-RFP and GFP tagged Piwi (Piwi::GFP) during AM lineage reprogramming. Whereas Piwi::GFP cannot be detected in the forming AMDCs during fragmentation of the AMs (F and F'), the VLM progenitor cells that arises from the AMDCs during reprogramming are clearly positive for cytoplasmic Piwi::GFP (G and G'). (H and H') Forced expression of constitutive active Hpo with org-1-GAL4 (org-1>>hpo.ΔC) abolishes piwi::GFP expression in pupal stage P4.

et al., 2016). Both signaling pathways have also been implicated in dedifferentiation processes: active JNK in germline cells (Herrera and Bach, 2018), and Hippo (specifically, inactive Wts) in retinal cells (Nicolay et al., 2010). We describe a novel, synergistic function of these two pathways in a specific type of muscle and connect them to lineage plasticity. Our data imply that the synergistic action of these two pathways in AM dedifferentiation is exerted predominantly in parallel at the level of their nuclear effectors, namely nuclear Yki/Sd, which requires inactivity of Hpo/Wts, and AP-1, which requires active JNK. Additionally, our data indicate that there is cross-regulation in which JNK also contributes to Yki activation, as has been described in studies on regeneration and size regulation in wing discs. As proposed for the wing disc, this input may involve inactivation of Wts upon JNK activation (Sun and Irvine, 2013; Willsey et al., 2016). The synergistic activities of the nuclear effectors of the Hippo and JNK cascades could operate directly at the level of joint target genes. Our genetic data and expression analysis implicate Myc and piwi as important examples of such targets, which in turn are required for mediating downstream effects of the Hippo and JNK cascades during this naturally occurring reprogramming process. In future studies, it should be examined whether these putative target genes contain combinatorial binding sites for Sd and AP-1.

Related signaling inputs across species and other tissues during dedifferentiation and redifferentiation

Given that forced YAP expression can induce reprogramming of adult mammalian cells into cells with lineage progenitor characteristics (Panciera et al., 2016); that the consensus motif for AP-1 and TEAD transcription factors are both significantly enriched in YAP-binding regions in cancer cell lines (Zanconato et al., 2015); and that the induction of pluripotent stem cells requires the active JNK signaling pathway, c-Myc, and involves up-regulation of mili (piwil2, a mouse homologue of Drosophila piwi; Takahashi and Yamanaka, 2006; Mikkelsen et al., 2008; Neganova et al., 2016), we propose that the key components that drive AM muscle lineage reprogramming have broader, evolutionarily conserved roles in mediating lineage plasticity. Specifically with regard to muscle tissues, it is worth noting in this context that in activated mouse satellite cells, YAP expression surges, activated YAP protein promotes their proliferation and inhibits their differentiation, and conditional YAP knockout in these muscle stem cells curtails muscle regeneration (Judson et al., 2012; Sun et al., 2017). Likewise, in the mouse heart, conditional depletion of the activity of the Hippo pathway kinases by various means, or expression of activated YAP, promotes heart regeneration beyond the early postnatal stages it is normally limited to. These effects involve dedifferentiation, reversal to a fetal gene expression program, and proliferation of cardiomyocytes (Liu and Martin, 2019). Although the role of Hippo inactivation and Yki/YAP activation in tissue growth has been amply documented, these and other findings reinforce the

Scale bars in A, B, and E: 100 $\mu m;$ C, D, and F–H: 10 $\mu m.$ Actin is visualized with phalloidin; DNA is visualized with DAPI.



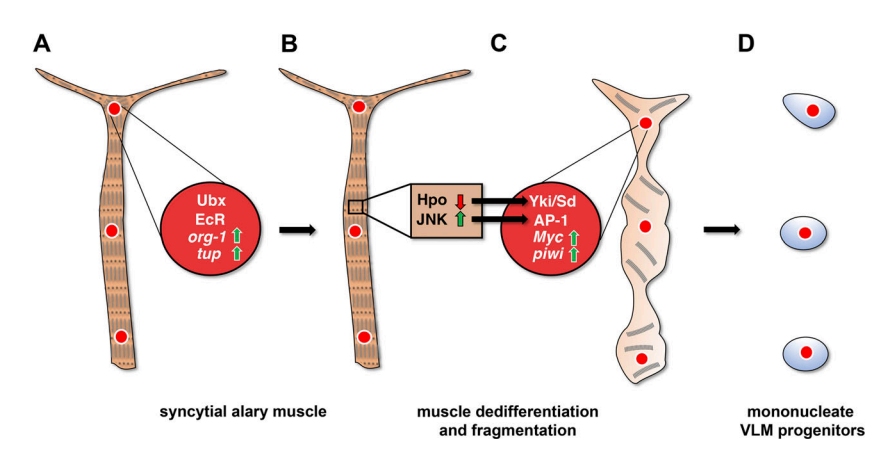


Figure 5. Lineage-restricted activation of Yki and JNK triggers dedifferentiation and reprogramming of syncytial AMs into VLM progenitor cells. (A) AM lineage reprogramming is induced by the nuclear activities of Ultrabithorax (Ubx) and ligand bound ecdysone receptor, thus leading to the up-regulation of org-1 and tup expression. (B) Subsequently, Org-1 and Tup promote the derepression of Yki via down-regulation of Hippo (Hpo) as well as the activation of JNK signaling. (C and **D)** These molecular events mediate the nuclear translocation of Yki/Sd as well as AP-1 and provoke lineagerestricted activation of Myc and piwi expression, inducing the dedifferentiation and fragmentation of the AMs into AM-derived cells (AMDCs; C) as well as the reprogramming of the AMDCs into mononucleate VLM progenitors (D). piwi is required for their redifferentiation into VLMs (not depicted).

notion that, depending on the context, this pathway can also exert cellular dedifferentiation. Of note, in the tissue context examined herein, the dedifferentiated AMDCs do not proliferate; instead, upon being reprogrammed into founder cells of the VLMs, they directly undergo myoblast fusion with fusion-competent myoblasts that have multiplied and migrated from lateral sources (Schaub et al., 2015). Nevertheless, the intriguing parallels in the roles of inactive Hippo/active Yki/YAP in promoting Drosophila AM and mouse cardiomyocyte dedifferentiation, as well as in maintaining the dedifferentiated state of mouse muscle stem cells, warrant the search for additional similarities, including the potential involvement of regulatory inputs and outputs described in our current study, in muscle and heart regeneration in the mouse and other vertebrate models.

Like Hippo inactivation, Myc function is mainly known for promoting proliferation and growth. However, besides these roles it has been connected to the induction of proapoptotic genes in a cell-autonomous as well as a non-cell-autonomous manner (McMahon, 2014). Conversely, it can also exhibit antiapoptotic and proautophagic effects in cancer cells (Conacci-Sorrell et al., 2014). We infer that Myc activation during AM lineage reprogramming is instrumental in initiating the mechanistic apparatus that executes the dedifferentiation and fragmentation process. This may include the induction of the nonapoptotic activity of caspases as well as of autophagic genes involved in the disintegration of AM muscle components and syncytial fragmentation. We show that cytoplasmic Piwi function is crucially required in the generated AMDCs to proceed with transdifferentiation. Cytoplasmic expression of PIWI proteins is associated with lineage-restricted somatic stem cells from Hydra to mammals, and there seems to be a strong correlation between PIWI expression and plasticity (van Wolfswinkel, 2014). Accordingly, we envision that Piwi function in the AMDCs may be involved in the suppression of AM lineage-specific programs. This could provide increased plasticity as a prerequisite for the reprogramming of AMDCs into VLM progenitor cells. Rather than being involved in the suppression of transposable elements, it is more likely that Piwi functions through the degradation of cellular mRNAs during this process, which is also compatible with its observed cytoplasmic localization in the VLM progenitors. Precedence for this type of

function exists, for example, in the Piwi-mediated degradation of a large set of uniformly distributed maternal transcripts around the onset of zygotic transcription in the early Drosophila embryo; the degradation of mRNAs (and long noncoding RNAs) during consecutive steps of spermatogenesis in the mouse via different PIWI family members so that development can transition to the next steps of meiosis and spermiogenesis; and the degradation of cellular mRNAs via Piwi in somatic niche cells to advance their development during Drosophila oogenesis (Rouget et al., 2010; Rojas-Ríos and Simonelig, 2018). Intriguingly, one important target of Piwi during this latter process is dFos mRNA, which needs to be destabilized for enabling the somatic niche cells to normally differentiate into follicle cells (Klein et al., 2016). It is thus conceivable that in AMDCs, Piwi exerts a negative feedback and destabilizes dFos, among other AM or dedifferentiationspecific mRNAs, to allow the transition toward the VLM progenitor fate.

Taking these observations together, we suggest a mechanism in which Org-1/Tup-driven lineage-restricted activation of Yki as well as JNK in the AMs triggers a mechanism that executes cellular reprogramming and whose key components have evolutionarily conserved roles (Fig. 5). Further dissection of this transdifferentiation process occurring naturally in vivo will uncover additional components linking these regulatory pathways and mediating muscle cell plasticity, which may also shed more light on general mechanisms of lineage plasticity and cellular reprogramming.

Materials and methods

Drosophila stocks

Standard Drosophila genetics was performed at 25°C. The following stocks were used: TRE-GFP (Chatterjee and Bohmann, 2012), UAS-hpo, UAS-hpo.delta.N, UAS-hpo.delta.C, UAS-hpo.delta.CK7IR (Jia et al., 2003), UAS-aPKC.CAAX.DN (Sotillos et al., 2004), hand-GFP (Sellin et al., 2006), org-1-GAL4 (line S18), org-1-RFP (Schaub et al., 2015). UAS-dsRNA-yki (34067), UAS-dsRNA-sd (55404), UAS-dsRNA-Jra (31595), UAS-dsRNA-kay (33379), UAS-dsRNA-Myc (51454), UAS-dsRNA-piwi-1 (33724), UAS-dsRNA-piwi-2 (34866), UAS-dsRNA-org-1 (62953), UAS-dsRNA-tup (51763), UAS-yki.S168A (28816), UAS-bsk.DN (6409), UAS-aPKC.CA (51673), UAS-Cas9.P2

3578



Table 1. Sequences of gRNAs

gRNA	Sequence (5' to 3')
sd_gRNA_1 X:1582001515820037 (+ strand)	CCGCTGATGCCGAAGGTGTATGG
sd_gRNA_2 X:1582007115820093 (+ strand)	TTATCTATATATCCGCCGTGCGG
sd_gRNA_3 X:1582011315820135 (+ strand)	TCCGACGAGGGTAAAATGTACGG
sd_gRNA_4 X:1581961915819641 (+ strand)	CCGTGGACACCAGTGAATGCCGG
yki_gRNA_1 2R:2406808124068103 (- strand)	ATTCGACAGCGTCCTGAATCCGG
yki_gRNA_2 2R:2406806924068091 (+ strand)	GCTTGGCGTCACCCGGATTCAGG
yki_gRNA_3 2R:2406796124067983 (- strand)	CGCCGACTCCACCTACGACGCGG
yki_gRNA_4 2R:2406795324067975 (+ strand)	CTGGGAGCCCGCGTCGTAGGTGG
Jra_gRNA_1 2R:1009737710097399 (- strand)	ACTGAAAGTCCAGTGACATGGGG
Jra_gRNA_2 2R:1009751310097535 (- strand)	ACCGTCTTGGATGACAGATCCGG
Jra_gRNA_3 2R:1009742110097443 (- strand)	GGGACGCTTGTTAGGATTCGGGG
Jra_gRNA_4 2R:1009734510097367 (+ strand)	ATACCTAAAACCGAGCCCGTTGG
kay_gRNA_1 3R:2979141329791435 (- strand)	TCGTCAGTGTGAGAACACTCTGG
kay_gRNA_2 3R:2979145729791479 (- strand)	TGTGTCCTCGATGTTGCGCGTGG
kay_gRNA_3 3R:2979148529791507 (- strand)	TCTGCGTGTCCGAGAGCAAGTGG
kay_gRNA_4 3R:2979151029791532 (+ strand)	GATCGTGTGGCTGGTTGCGCGGG
Myc_gRNA_1 X:33750273375049 (- strand)	TGGTCGTCCATTATGGAATACGG
Myc_gRNA_2 X:33751243375146 (- strand)	CTTCTCGAGATCACTCTGAATGG
Myc_gRNA_3 X:33755373375559 (+ strand)	GAGGTCCATTTAATACCGCCCGG
Myc_gRNA_4 X:33759783376000 (- strand)	CTATCAGAGCCGGTCGTCGGCGG

(58986), sd::GFP (50827), and Myc::GFP (81274) were obtained from the Bloomington Drosophila Stock Center. yki::GFP (318237) and piwi::GFP (313319) were obtained from the Vienna Drosophila Resource Center.

Generation of transgenic Drosophila stocks

We used the system described in Port and Bullock (2016) to create UAS inducible and t::gRNA array expressing transgenes. We amplified PCR fragments with the respective primers containing the gRNA sequences (Table 1) and 1 ng pCFD6 (Addgene, 73915) as template using Q5 Hot Start High-Fidelity 2X Master Mix (New England Biolabs, M0494L). The PCR fragments were gel purified using the QIAquick Gel Extraction Kit (Qiagen, 28704), and the respective constructs were assembled with BbsI-HF (New England Biolabs, 3539S) digested pCFD6 backbone using the NEBuilder HiFi DNA Assembly Cloning Kit (New England Biolabs, R5520S), following the instructions provided by the manufacturers.

Sequences of gRNAs (Table 1) and primers (Table 2) used for the assembly of the respective pCFD6 construct gRNAs were obtained from https://www.flyrnai.org/crispr/. Transgenes of the respective pCFD6 constructs were generated by a commercial embryo injection service (BestGene, Chino Hills, CA) using the phiC31/attP/attB system (Bischof et al., 2007) at the attP40 (UAS-t::gRNA-yki^{4x}, UAS-t::gRNA-Jra^{4x}), attP2 (UAS-t::gRNA-kay^{4x}, UAS-t::gRNA-Myc^{4x}), and VK00027 (UAS-t::gRNA-sd^{4x}) landing sites. Potential transformants were selected by mini-white expression.

Fluorescent antibody staining

Dissections of pupal stages until P4 (for pupal staging, see Bainbridge and Bownes [1981]) were performed after prefixation with 3.7% formaldehyde for 30 min with microsurgery scissors in toto. To dissect pharate adult stages, the pupal cases were removed before prefixation. For antibody stainings, the dissected animals were fixed in 3.7% formaldehyde for 10 min, washed three times for 30 min in PBT (PBS + 0.1% Tween 20), blocked in 10% BSA (Serva, 11930.04) for 1 h, and incubated with the primary antibodies, goat polyclonal anti-GFP (GeneTex, GTX26673, 1:1,000) and rabbit polyclonal anti-RFP (Rockland, 600-401-379S, 1:500) for 2 d at 4°C. To visualize filamentous actin, Atto 647N-conjugated phalloidin (1:1,000, Sigma-Aldrich, 65906) was added to the antibody solution. After incubation with the primary antibodies, the dissections were washed three times for 30 min in PBT and incubated with the respective secondary antibodies, Alexa Fluor 488-conjugated donkey antigoat (Abcam, ab150129) and Alexa Fluor 555-conjugated donkey anti-rabbit (Abcam, ab150074), in 1:200 dilution overnight at 4°C. Finally, the stained animals were washed three times for 30 min in PBT and embedded into Vectashield containing DAPI (Vectorlabs, H-1200).

Fixed sample analysis

Confocal Z-stacks of fixed specimens were acquired with a Leica SP5 II ($20 \times /0.7$ HC PL APO Glycerol, $63 \times /1.3$ HC PL APO Glycerol). Maximum projections of the Z-stacks were performed with Leica Application Suite X (Leica Microsystems).

3580



Table 2. Primers used for the assembly of the respective pCFD6 construct gRNAs

Primer	Sequence (5' to 3')
sd_PCR1F	CGGCCCGGGTTCGATTCCCGGCCGATGCACCGCTGATGCCGAAGGTGTAGTTTCAGAGCTATGCTGGAAAC
sd_PCR1R	CACGGCGGATATATAGATAATGCACCAGCCGGGAATCGAACC
sd_PCR2F	TTATCTATATATCCGCCGTGGTTTCAGAGCTATGCTGGAAAC
sd_PCR2R	TACATTTTACCCTCGTCGGATGCACCAGCCGGGAATCGAACC
sd_PCR3F	TCCGACGAGGGTAAAATGTAGTTTCAGAGCTATGCTGGAAAC
sd_PCR3R	ATTTTAACTTGCTATTTCTAGCTCTAAAACGCATTCACTGGTGTCCACGGTGCACCAGCCGGGAATCGAACC
yki_PCR1F	CGGCCCGGGTTCGATTCCCGGCCGATGCAATTCGACAGCGTCCTGAATCGTTTCAGAGCTATGCTGGAAAC
yki_PCR1R	GAATCCGGGTGACGCCAAGCTGCACCAGCCGGGAATCGAACC
yki_PCR2F	GCTTGGCGTCACCCGGATTCGTTTCAGAGCTATGCTGGAAAC
yki_PCR2R	CGTCGTAGGTGGAGTCGGCGTGCACCAGCCGGGAATCGAACC
yki_PCR3F	CGCCGACTCCACCTACGACGGTTTCAGAGCTATGCTGGAAAC
yki_PCR3R	ATTTTAACTTGCTATTTCTAGCTCTAAAACCCTACGACGCGGGCTCCCAGTGCACCAGCCGGGAATCGAACC
Jra_PCR1F	CGGCCCGGGTTCGATTCCCGGCCGATGCAACTGAAAGTCCAGTGACATGGTTTCAGAGCTATGCTGGAAAC
Jra_PCR1R	GATCTGTCATCCAAGACGGTTGCACCAGCCGGGAATCGAACC
Jra_PCR2F	ACCGTCTTGGATGACAGATCGTTTCAGAGCTATGCTGGAAAC
Jra_PCR2R	CGAATCCTAACAAGCGTCCCTGCACCAGCCGGGAATCGAACC
Jra_PCR3F	GGGACGCTTGTTAGGATTCGGTTTCAGAGCTATGCTGGAAAC
Jra_PCR3R	ATTTTAACTTGCTATTTCTAGCTCTAAAACACGGGCTCGGTTTTAGGTATTGCACCAGCCGGGAATCGAACC
kay_PCR1F	CGGCCCGGGTTCGATTCCCGGCCGATGCATCGTCAGTGTGAGAACACTCGTTTCAGAGCTATGCTGGAAAC
kay_PCR1R	CGCGCAACATCGAGGACACATGCACCAGCCGGGAATCGAACC
kay_PCR2F	TGTGTCCTCGATGTTGCGCGGTTTCAGAGCTATGCTGGAAAC
kay_PCR2R	CTTGCTCTCGGACACGCAGATGCACCAGCCGGGAATCGAACC
kay_PCR3F	TCTGCGTGTCCGAGAGCAAGGTTTCAGAGCTATGCTGGAAAC
kay_PCR3R	ATTTTAACTTGCTATTTCTAGCTCTAAAACGCGCAACCAGCCACACGATCTGCACCAGCCGGGAATCGAACC
Myc_PCR1F	CGGCCCGGGTTCGATTCCCGGCCGATGCATGGTCGTCCATTATGGAATAGTTTCAGAGCTATGCTGGAAAC
Myc_PCR1R	TTCAGAGTGATCTCGAGAAGTGCACCAGCCGGGAATCGAACC
Myc_PCR2F	CTTCTCGAGATCACTCTGAAGTTTCAGAGCTATGCTGGAAAC
Myc_PCR2R	GGCGGTATTAAATGGACCTCTGCACCAGCCGGGAATCGAACC
Myc_PCR3F	GAGGTCCATTTAATACCGCCGTTTCAGAGCTATGCTGGAAAC
Myc_PCR3R	ATTTTAACTTGCTATTTCTAGCTCTAAAACCCGACGACCGGCTCTGATAGTGCACCAGCCGGGAATCGAACC

In vivo time-lapse imaging

Stage P3 pupae of the respective genotypes were aligned on a strip of double-faced adhesive tape connected to a slide and covered with a drop of Halocarbon oil 700 (Halocarbon Products Corp., Sigma-Aldrich, H8898) and a coverslip. Time-lapse series were acquired on a Leica SP5 II confocal system using a HC PL APO $10\times/0.4$ Air. Acquisition was done over a time course of 15–20 h with the following settings: pinhole 1.4 AU; 1.5× optical zoom, scan speed 200 Hz, line averaging 3, and Z-stack ~20 sections with a step size of 3 μ m and time intervals of 10 min per stack. Videos were generated using Leica Application Suite X and further processed with Photoshop CS6 (Adobe Systems).

Statistical analysis

For quantification of the VLM phenotype frequency, living adult pharate stages of the respective genotypes were aligned

on a microscope slide. The org-1-HN18-RFP lineage marker in the living animals was visualized with the aid of a fluorescence-equipped microscope (Nikon, Eclipse 80i), and phenotypic classification was performed by morphological analysis of the RFP-positive cells. Pharate adult stages with differentiated VLM were defined by the presence of RFPpositive elongated muscle fibers that were ventrally attached to the adult heart and resembled the typical elongated VLM morphology. Pharate adult stages with no differentiated VLM were defined by the presence of either RFP-positive AMs (not being dedifferentiated) or spherical RFP-positive (muscle) cells. These phenotypic classes were scored relative to each other, and frequencies were calculated (Table S1). Statistical analysis of the samples was performed with the χ^2 test function of Excel (Microsoft). Statistical significance was defined by $P \le 0.05$.



Online supplemental material

Fig. S1 shows that induction of RNAi against the transcriptional effectors of Hpo and JNK, as well as the Yki target Myc, abolishes VLM differentiation in pharate adult stages. Table S1 shows the respective observed phenotypic frequencies of the genetic experiments. Video 1 shows the alary muscle lineage reprogramming process in a wild-type pupa. Video 2 demonstrates inhibition of alary muscle fragmentation in a *yki* compromised pupa. Video 3 shows inhibition of alary muscle fragmentation in a *Myc* compromised pupa. Video 4 demonstrates that loss of *piwi* function provokes arrest of transdifferentiation after alary muscle fragmentation..

Acknowledgments

We are grateful to Johannes März for helping us with dissections. We thank the *Drosophila* community for supplying us with fly stocks, in particular Dirk Bohmann (University of Rochester Medical Center, Rochester, NY), Sonsoles Campuzano (CBM Severo Ochoa, Madrid, Spain), Fillip Port (DKFZ, Heidelberg, Germany) and Jin Jiang (UT Southwestern Medical Center, Dallas, TX), as well as the Vienna *Drosophila* Resource Center and the Bloomington *Drosophila* Stock Center.

This work was funded by grants from the Deutsche Forschungsgemeinschaft to C. Schaub (SCHA 2091/1-1) and M. Frasch (FR 696/6-1) and was supported by the Optical Imaging Centre Erlangen.

The authors declare no competing financial interests.

Author contributions: Conceptualization: C. Schaub and M. Frasch; Investigation: C. Schaub and M. Rose; Writing – Original Draft: C. Schaub; Writing – Review & Editing: C. Schaub and M. Frasch; Funding Acquisition: C. Schaub and M. Frasch; Supervision: C. Schaub.

Submitted: 7 May 2019 Revised: 16 August 2019 Accepted: 20 August 2019

References

- Bainbridge, S.P., and M. Bownes. 1981. Staging the metamorphosis of Drosophila melanogaster. *J. Embryol. Exp. Morphol.* 66:57–80.
- Bischof, J., R.K. Maeda, M. Hediger, F. Karch, and K. Basler. 2007. An optimized transgenesis system for Drosophila using germ-line-specific phiC31 integrases. Proc. Natl. Acad. Sci. USA. 104:3312–3317. https://doi.org/10.1073/pnas.0611511104
- Chatterjee, N., and D. Bohmann. 2012. A versatile ΦC31 based reporter system for measuring AP-1 and Nrf2 signaling in Drosophila and in tissue culture. *PLoS One.* 7:e34063. https://doi.org/10.1371/journal.pone.0034063
- Conacci-Sorrell, M., C. Ngouenet, S. Anderson, T. Brabletz, and R.N. Eisenman. 2014. Stress-induced cleavage of Myc promotes cancer cell survival. Genes Dev. 28:689–707. https://doi.org/10.1101/gad.231894.113
- Dobi, K.C., V.K. Schulman, and M.K. Baylies. 2015. Specification of the somatic musculature in Drosophila. Wiley Interdiscip. Rev. Dev. Biol. 4: 357–375. https://doi.org/10.1002/wdev.182
- Dutta, D., and K. VijayRaghavan. 2006. Metamorphosis and the Formation of the Adult Musculature. *In H. Sink*, editor. *Muscle Development in Drosophila*.Springer Science + Business Media, New York; 125-142.
- Frasch, M. 2016. Dedifferentiation, Redifferentiation, and Transdifferentiation of Striated Muscles During Regeneration and Development. Curr. Top. Dev. Biol. 116:331–355. https://doi.org/10.1016/bs.ctdb .2015.12.005

- Goulev, Y., J.D. Fauny, B. Gonzalez-Marti, D. Flagiello, J. Silber, and A. Zider. 2008. SCALLOPED interacts with YORKIE, the nuclear effector of the hippo tumor-suppressor pathway in Drosophila. Curr. Biol. 18:435–441. https://doi.org/10.1016/j.cub.2008.02.034
- Grzeschik, N.A., L.M. Parsons, M.L. Allott, K.F. Harvey, and H.E. Richardson. 2010. Lgl, aPKC, and Crumbs regulate the Salvador/Warts/Hippo pathway through two distinct mechanisms. *Curr. Biol.* 20:573–581. https://doi.org/10.1016/j.cub.2010.01.055
- Gunage, R.D., N. Dhanyasi, H. Reichert, and K. VijayRaghavan. 2017. Drosophila adult muscle development and regeneration. Semin. Cell Dev. Biol. 72:56-66. https://doi.org/10.1016/j.semcdb.2017.11.017
- Harvey, K.F., C.M. Pfleger, and I.K. Hariharan. 2003. The Drosophila Mst ortholog, hippo, restricts growth and cell proliferation and promotes apoptosis. Cell. 114:457–467. https://doi.org/10.1016/S0092-8674(03) 00557-9
- Herrera, S.C., and E.A. Bach. 2018. JNK signaling triggers spermatogonial dedifferentiation during chronic stress to maintain the germline stem cell pool in the *Drosophila* testis. *eLife*. 7:e36095. https://doi.org/10.7554/eLife.36095
- Huang, J., S. Wu, J. Barrera, K. Matthews, and D. Pan. 2005. The Hippo signaling pathway coordinately regulates cell proliferation and apoptosis by inactivating Yorkie, the Drosophila Homolog of YAP. Cell. 122: 421–434. https://doi.org/10.1016/j.cell.2005.06.007
- Jia, J., W. Zhang, B. Wang, R. Trinko, and J. Jiang. 2003. The Drosophila Ste20 family kinase dMST functions as a tumor suppressor by restricting cell proliferation and promoting apoptosis. Genes Dev. 17:2514–2519. https://doi.org/10.1101/gad.1134003
- Judson, R.N., A.M. Tremblay, P. Knopp, R.B. White, R. Urcia, C. De Bari, P.S. Zammit, F.D. Camargo, and H. Wackerhage. 2012. The Hippo pathway member Yap plays a key role in influencing fate decisions in muscle satellite cells. J. Cell Sci. 125:6009-6019. https://doi.org/10.1242/jcs.109546
- Jung, D.W., and D.R. Williams. 2011. Novel chemically defined approach to produce multipotent cells from terminally differentiated tissue syncytia. ACS Chem. Biol. 6:553–562. https://doi.org/10.1021/cb2000154
- Klein, J.D., C. Qu, X. Yang, Y. Fan, C. Tang, and J.C. Peng. 2016. c-Fos Repression by Piwi Regulates Drosophila Ovarian Germline Formation and Tissue Morphogenesis. PLoS Genet. 12:e1006281. https://doi.org/10.1371/journal.pgen.1006281
- Kockel, L., J.G. Homsy, and D. Bohmann. 2001. Drosophila AP-1: lessons from an invertebrate. Oncogene. 20:2347–2364. https://doi.org/10.1038/sj.onc .1204300
- Kuleesha, Y., W.C. Puah, and M. Wasser. 2016. A model of muscle atrophy based on live microscopy of muscle remodelling in Drosophila metamorphosis. R. Soc. Open Sci. 3:150517. https://doi.org/10.1098/rsos .150517
- LaBeau, E.M., D.L. Trujillo, and R.M. Cripps. 2009. Bithorax complex genes control alary muscle patterning along the cardiac tube of Drosophila. Mech. Dev. 126:478–486. https://doi.org/10.1016/j.mod.2009.01.001
- Liu, S., and J.F. Martin. 2019. The regulation and function of the Hippo pathway in heart regeneration. Wiley Interdiscip. Rev. Dev. Biol. 8:e335. https://doi.org/10.1002/wdev.335
- Llado, V., Y. Nakanishi, A. Duran, M. Reina-Campos, P.M. Shelton, J.F. Linares, T. Yajima, A. Campos, P. Aza-Blanc, M. Leitges, et al. 2015. Repression of Intestinal Stem Cell Function and Tumorigenesis through Direct Phosphorylation of β-Catenin and Yap by PKCζ. Cell Reports. 10: 740–754. https://doi.org/10.1016/j.celrep.2015.01.007
- McGann, C.J., S.J. Odelberg, and M.T. Keating. 2001. Mammalian myotube dedifferentiation induced by newt regeneration extract. Proc. Natl. Acad. Sci. USA. 98:13699-13704. https://doi.org/10.1073/pnas.221297398
- McMahon, S.B. 2014. MYC and the control of apoptosis. *Cold Spring Harb*. Perspect. Med. 4:a014407. https://doi.org/10.1101/cshperspect.a014407
- Mikkelsen, T.S., J. Hanna, X. Zhang, M. Ku, M. Wernig, P. Schorderet, B.E. Bernstein, R. Jaenisch, E.S. Lander, and A. Meissner. 2008. Dissecting direct reprogramming through integrative genomic analysis. *Nature*. 454:49–55. https://doi.org/10.1038/nature07056
- Neganova, I., E. Shmeleva, J. Munkley, V. Chichagova, G. Anyfantis, R. Anderson, J. Passos, D.J. Elliott, L. Armstrong, and M. Lako. 2016. JNK/SAPK Signaling Is Essential for Efficient Reprogramming of Human Fibroblasts to Induced Pluripotent Stem Cells. Stem Cells. 34:1198–1212. https://doi.org/10.1002/stem.2327
- Neto-Silva, R.M., S. de Beco, and L.A. Johnston. 2010. Evidence for a growth-stabilizing regulatory feedback mechanism between Myc and Yorkie, the Drosophila homolog of Yap. *Dev. Cell.* 19:507–520. https://doi.org/10.1016/j.devcel.2010.09.009

3582



- Nicolay, B.N., B. Bayarmagnai, N.S. Moon, E.V. Benevolenskaya, and M.V. Frolov. 2010. Combined inactivation of pRB and hippo pathways induces dedifferentiation in the Drosophila retina. *PLoS Genet.* 6: e1000918. https://doi.org/10.1371/journal.pgen.1000918
- Odelberg, S.J., A. Kollhoff, and M.T. Keating. 2000. Dedifferentiation of mammalian myotubes induced by msx1. *Cell*. 103:1099–1109. https://doi.org/10.1016/S0092-8674(00)00212-9
- Panciera, T., L. Azzolin, A. Fujimura, D. Di Biagio, C. Frasson, S. Bresolin, S. Soligo, G. Basso, S. Bicciato, A. Rosato, et al. 2016. Induction of Expandable Tissue-Specific Stem/Progenitor Cells through Transient Expression of YAP/TAZ. Cell Stem Cell. 19:725–737. https://doi.org/10.1016/j.stem.2016.08.009
- Pantalacci, S., N. Tapon, and P. Léopold. 2003. The Salvador partner Hippo promotes apoptosis and cell-cycle exit in Drosophila. Nat. Cell Biol. 5: 921-927. https://doi.org/10.1038/ncb1051
- Port, F., and S.L. Bullock. 2016. Augmenting CRISPR applications in Drosophila with tRNA-flanked sgRNAs. Nat. Methods. 13:852–854. https://doi.org/10.1038/nmeth.3972
- Rojas-Ríos, P., and M. Simonelig. 2018. piRNAs and PIWI proteins: regulators of gene expression in development and stem cells. *Development*. 145: dev161786. https://doi.org/10.1242/dev.161786
- Rouget, C., C. Papin, A. Boureux, A.C. Meunier, B. Franco, N. Robine, E.C. Lai, A. Pelisson, and M. Simonelig. 2010. Maternal mRNA deadenylation and decay by the piRNA pathway in the early Drosophila embryo. *Nature*. 467:1128–1132. https://doi.org/10.1038/nature09465
- Sandoval-Guzmán, T., H. Wang, S. Khattak, M. Schuez, K. Roensch, E. Nacu, A. Tazaki, A. Joven, E.M. Tanaka, and A. Simon. 2014. Fundamental differences in dedifferentiation and stem cell recruitment during skeletal muscle regeneration in two salamander species. Cell Stem Cell. 14:174–187. https://doi.org/10.1016/j.stem.2013.11.007
- Schaub, C., J. März, I. Reim, and M. Frasch. 2015. Org-1-dependent lineage reprogramming generates the ventral longitudinal musculature of the Drosophila heart. Curr. Biol. 25:488-494. https://doi.org/10.1016/j.cub .2014.12.029
- Schulman, V.K., E.S. Folker, J.N. Rosen, and M.K. Baylies. 2014. Syd/JIP3 and JNK signaling are required for myonuclear positioning and muscle function. PLoS Genet. 10:e1004880. https://doi.org/10.1371/journal.pgen .1004880
- Sellin, J., S. Albrecht, V. Kölsch, and A. Paululat. 2006. Dynamics of heart differentiation, visualized utilizing heart enhancer elements of the Drosophila melanogaster bHLH transcription factor Hand. Gene Expr. Patterns. 6:360–375. https://doi.org/10.1016/j.modgep.2005.09.012
- Sotillos, S., M.T. Díaz-Meco, E. Caminero, J. Moscat, and S. Campuzano. 2004. DaPKC-dependent phosphorylation of Crumbs is required for epithelial cell polarity in Drosophila. J. Cell Biol. 166:549–557. https://doi.org/10 .1083/jcb.200311031

- Sun, G., and K.D. Irvine. 2013. Ajuba family proteins link JNK to Hippo signaling. Sci. Signal. 6:ra81. https://doi.org/10.1126/scisignal.2004324
- Sun, C., V. De Mello, A. Mohamed, H.P. Ortuste Quiroga, A. Garcia-Munoz, A. Al Bloshi, A.M. Tremblay, A. von Kriegsheim, E. Collie-Duguid, N. Vargesson, et al. 2017. Common and Distinctive Functions of the Hippo Effectors Taz and Yap in Skeletal Muscle Stem Cell Function. Stem Cells. 35:1958–1972. https://doi.org/10.1002/stem.2652
- Takahashi, K., and S. Yamanaka. 2006. Induction of pluripotent stem cells from mouse embryonic and adult fibroblast cultures by defined factors. *Cell*. 126:663–676. https://doi.org/10.1016/j.cell.2006.07.024
- Taniguchi, K., S. Hozumi, R. Maeda, M. Ooike, T. Sasamura, T. Aigaki, and K. Matsuno. 2007. D-JNK signaling in visceral muscle cells controls the laterality of the Drosophila gut. *Dev. Biol.* 311:251–263. https://doi.org/10.1016/j.ydbio.2007.08.048
- Udan, R.S., M. Kango-Singh, R. Nolo, C. Tao, and G. Halder. 2003. Hippo promotes proliferation arrest and apoptosis in the Salvador/Warts pathway. Nat. Cell Biol. 5:914–920. https://doi.org/10.1038/ncb1050
- van Wolfswinkel, J.C. 2014. Piwi and potency: PIWI proteins in animal stem cells and regeneration. *Integr. Comp. Biol.* 54:700–713. https://doi.org/10.1093/jcb/jcu084
- Willsey, H.R., X. Zheng, J. Carlos Pastor-Pareja, A.J. Willsey, P.A. Beachy, and T. Xu. 2016. Localized JNK signaling regulates organ size during development. eLife. 5:e11491. https://doi.org/10.7554/eLife.11491
- Wu, S., Y. Liu, Y. Zheng, J. Dong, and D. Pan. 2008. The TEAD/TEF family protein Scalloped mediates transcriptional output of the Hippo growthregulatory pathway. *Dev. Cell.* 14:388–398. https://doi.org/10.1016/j .devcel.2008.01.007
- Zanconato, F., M. Forcato, G. Battilana, L. Azzolin, E. Quaranta, B. Bodega, A. Rosato, S. Bicciato, M. Cordenonsi, and S. Piccolo. 2015. Genome-wide association between YAP/TAZ/TEAD and AP-1 at enhancers drives oncogenic growth. Nat. Cell Biol. 17:1218–1227. https://doi.org/10.1038/ncb3216
- Zhang, C., B.S. Robinson, W. Xu, L. Yang, B. Yao, H. Zhao, P.K. Byun, P. Jin, A. Veraksa, and K.H. Moberg. 2015. The ecdysone receptor coactivator Taiman links Yorkie to transcriptional control of germline stem cell factors in somatic tissue. *Dev. Cell.* 34:168–180. https://doi.org/10.1016/j.devcel.2015.05.010
- Zhao, B., X. Ye, J. Yu, L. Li, W. Li, S. Li, J. Yu, J.D. Lin, C.Y. Wang, A.M. Chinnaiyan, et al. 2008. TEAD mediates YAP-dependent gene induction and growth control. *Genes Dev.* 22:1962–1971. https://doi.org/10.1101/gad.1664408
- Ziosi, M., L.A. Baena-López, D. Grifoni, F. Froldi, A. Pession, F. Garoia, V. Trotta, P. Bellosta, S. Cavicchi, and A. Pession. 2010. dMyc functions downstream of Yorkie to promote the supercompetitive behavior of hippo pathway mutant cells. PLoS Genet. 6:e1001140. https://doi.org/10.1371/journal.pgen.1001140